arXiv:1409.4655v2 [nucl-ex] 19 Sep 2014

Proceedings of the Second Annual LHCP

September 22, 2014

Jet Production in p-Pb Collisions

Megan Connors

On behalf of the ALICE Collaboration,
Department of Physics
Yale University, New Haven, CT 06511, U.S.A.

ABSTRACT

One of the major results from the study of high energy heavy ion collisions is the observation of jet quenching. The suppression of the number of jets observed in heavy ion collisions relative to pp collisions at the same energy scaled by the number of binary collisions, is attributed to partonic energy loss in the quark gluon plasma (QGP). However, cold nuclear matter effects due to the presence of a nucleus in the initial state could also influence this measurement. To disentangle these effects p-Pb collisions are studied, where QGP formation is not expected to occur and only cold nuclear matter effects are present. In addition to being an important baseline for understanding jet quenching, jets in p-Pb collisions may also be used to provide constraints on the nuclear parton distribution functions. Fully reconstructed jets measured using the ALICE tracking system and electro-magnetic calorimeter in p-Pb collisions at $\sqrt{s_{NN}} = 5.02$ TeV are reported. In addition to the spectra, studies of the jet fragmentation behavior in p-Pb collisions are also presented.

PRESENTED AT

The Second Annual Conference
on Large Hadron Collider Physics
Columbia University, New York, U.S.A
June 2-7, 2014

1 Introduction

Heavy ions collisions at high energies produce a state of matter called the Quark Gluon Plasma (QGP). Jets are an excellent probe of the QGP, since they originate from hard scatterings early in the collision. As the produced parton traverses the QGP, it loses energy. The result is jet quenching, which has been observed and is quantified by comparing the fully corrected jet spectrum measured in central Pb-Pb collisions to that measured in pp scaled by the average number of binary collisions, $\langle N_{\rm coll} \rangle$ [1]. However, since the parton experiences all stages of the collision, cold nuclear matter (CNM) effects could also influence this measurement. Measuring the jet cross section in p-Pb collisions, which experience CNM effects without the QGP, is critical for disentangling initial and final state effects on the observed Pb-Pb jet spectra.

In addition to modifications of the total jet production, CNM could also influence the observed jet fragmentation. To study the fragmentation properties of the jet, the spectra for jets reconstructed at different radii are compared. A modification to the jet substructure would be observed if their ratio in p-Pb differs from the same ratio measured in pp collisions. However to further quantify the fragmentation behavior, the j_T, which is the vector between the charged track and the jet axis, is measured. The j_T distribution in p-Pb is then compared to PYTHIA.

Another important observation from heavy ion collisions has been the increased baryon to meson ratio for high multiplicity Pb-Pb collisions compared to low multiplicity events [2]. A similar behavior has been observed in p-Pb collisions [3]. For both systems, the Λ/K^0_s ratio for $p_T > 2$ GeV/c is higher for high multiplicity events than for low multiplicity events. In Pb-Pb, this observation has been attributed to radial flow. The applicability of hydrodynamics to smaller systems such as p-Pb is still under investigation. While this modification has been observed, it is unclear whether the composition of the jet is being modified or if it arises from soft (small Q^2) processes in the underlying event.

2 Analysis Details

Three independent analyses studing jets in the p-Pb collisions are presented: the fully reconstructed jet spectrum, the j_T distribution and the measurement of V^0 particles in charged jets. Since the methods used in these analyses overlap, a general discussion of the analysis details is presented. Cases where there are differences in the procedures are noted.

The presented analyses all use data collected by the ALICE experiment during the 5.02 TeV p-Pb LHC run from 2013. The jet spectrum and V^0 study use minimum bias p-Pb events corresponding to an integrated luminosity of $51\mu b^{-1}$ while the j_T study also incorporates events triggered by the electromagentic calorimeter (EMCal). Event multiplicity classes are determined using the VZERO-A detector which covers the psuedorapidity, $2.8 < \eta < 5.1$ in the Pb going direction. Charged tracks are measured in the ALICE central tracking system, which consists of the Time Projection Chamber (TPC) and a silicon Inner Tracking System (ITS). To account for the neutral energy of the jet, clusters are measured in the EMCal, which covers 110° in azimuth and $|\eta| < 0.7$. Clusters are corrected for energy deposited in the EMCal by charged tracks [4].

2.1 Jet Reconstruction and Underlying Event Correction

For full jet reconstruction EMCal clusters with $E_T > 300$ MeV and charged tracks with $p_T > 150$ MeV/c are input to the jet finding algorithm. Note that the jets in the V^0 study only include the charged tracks. Jets are reconstructed with the anti-k_T jet finding algorithm with various resolution parameters, R using the FastJet package [5]. To ensure the jet is fully within the acceptance, the jet axis must be at least R away from the edge of the detector. The V^0 measurement restricts the jets to $|\eta| < 0.75 - R$.

Energy from the underlying event is also clustered into the jets by the algorithm and must be subtracted from the total raw jet energy. An average energy density, ρ, is determined on an event-by-event basis and then subtracted from each jet in the event according to $p^{reco}_{T,jet} = p^{raw}_{T,jet} - \rho \times A_{jet}$ where A_{jet} is the area of the reconstructed jet. For the full jet analyses, the charged track p_T density, ρ^{ch}, which is measured in full azimuth is scaled using a scale factor that is determined from measured data to include electromagnetic

contributions, as done in the Pb-Pb jet spectra analysis [1]. The charged track background density, ρ^{ch}, is determined by the median occupancy method, a slightly modified implementation of the method presented in [6]. The median occupancy method, defined by

$$\rho^{ch} = \text{median}\left\{\frac{\mathrm{p_T^i}}{\mathrm{A_i}}\right\} \times \mathrm{C}, \tag{1}$$

is determined by running the k_T algorithm over all tracks plus "ghost particles" (fake particles with negligible momentum used by FastJet for the jet area calculation) in the event [5]. Before determining the median of the physical jets, any k_T jets overlapping with signal jets are excluded. The median is scaled by an occupancy correction factor, C, accounting for the emptiness of the p-Pb event. $C = A_{\mathrm{phys}}/A_{\mathrm{tot}}$, where A_{phys} is the area of all physical jets and A_{tot} is the area of all jets, including jets comprised of ghost particles only.

2.2 V^0 Candidate Selection and Underlying Event Correction

The Λ and K_s^0 candidates are reconstructed via their hadronic decay channels, $\Lambda \to p\pi^-$ and $K_s^0 \to \pi^+\pi^-$. The decay daughters are identificed in the TPC according to their specific ionization, $\mathrm{d}E/\mathrm{d}x$. A fiducial cut was applied requiring all V^0 particles satisfy $|\eta_{\mathrm{V}^0} < 0.75|$. Additional details can be found in [7].

V^0 candidates are considered to be part of a jet if the distance between the candidate and the jet axis is less than the resolution parameter, R. The number of V^0 candidates within the jet cone is corrected for the underlying event. To estimate the contribution from V^0 particles not associated with the hard scattering, V^0 particles are measured outside the jet cone and in non-jet events. The difference in the spectra from these two different selection criteria estimates the systematic uncertainty on the background determination. Feed-down of Λ from Ξ is corrected using the feed-down fraction of inclusive Λ determined from the data.

2.3 Unfolding

After background subtraction, the jet spectra must be corrected for detector effects and fluctuations in the underlying event. The effect of the detector on the spectra is determined by passing PYTHIA events at $\sqrt{s} =$ 5.02 TeV through a GEANT simulation of the ALICE detector. Jets reconstructed at the detector level are geometrically matched to the closest particle level jet. A 2-dimensional histogram or response matrix (RM) maps detector level jet p_T to particle level jet p_T. More details are available in [8].

The underlying event energy density, is determined on an event-by-event basis. However, the background energy density fluctuates within each event. These fluctuations can be quantified by measuring the δp_T distribution using the method of Random Cones (RC) according to

$$\delta p_T = p_T^{RC} - \pi R_{RC}^2 \times \rho, \tag{2}$$

where p_T^{RC}, is the total momentum within a cone of radius, R_{RC}, placed randomly in the event.

The final RM, the multiplication of the detector RM and the δp_T distribution, is input to the unfolding algorithm. The singular value decomposition (SVD) algorithm was chosen as the default for unfolding the spectrum [9]. A bin-by-bin correction procedure was applied for the j_T analysis. For the jet spectra measurement, the bin-by-bin method was also in good agreement with the other unfolding algorithms.

3 Results

The unfolded spectra for $R = 0.4$ and $R = 0.2$ are shown in Figure 1. The spectra are normalized per number of binary collision, $\langle N_{\mathrm{coll}} \rangle$, to make a direct comparison to the pp references. Since no data exists on pp collisions at $\sqrt{s} = 5.02$ TeV, we compare the p-Pb data to Monte Carlo simulations. The plot includes PYTHIA8, PYTHIA6 and POWHEG using 2 different parton distribution functions (PDF). The POWHEG calculations include uncertainties on the factorization and renormalization scales (13%) and the uncertainty in the PDF (6% for CTEQ and 9% for EPS). The ratios between the data and the different models are all consistent with one, which would suggest there are no cold nuclear matter effects to the jet spectrum.

However, the spread and uncertainty from these different references is significant and demonstrates the need for a data reference to better quantify the CNM effects or lack of effects on the jet spectrum. Despite this uncertainty, the p-Pb results clearly show that the strong suppression observed in the Pb-Pb is not purely due to initial state effects, but is rather a result of energy loss in the produced medium.

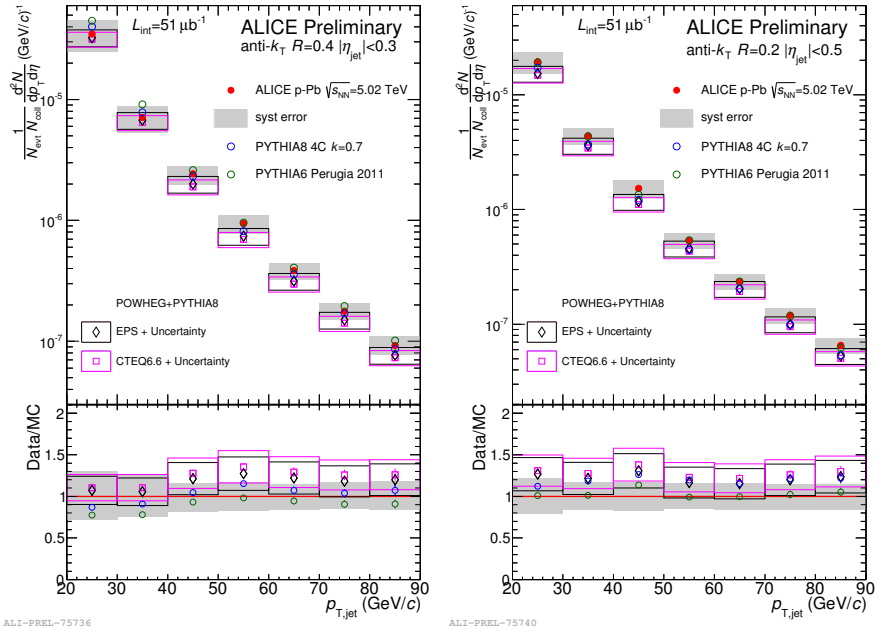

Figure 1: Fully corrected p-Pb jet spectrum for $R = 0.4$ and $R = 0.2$ scaled by $\langle N_{\mathrm{coll}} \rangle$ compared to PYTHIA and POWHEG simulations at 5.02 TeV.

Although the jet spectra appear unmodified, one may question whether the fragmentation could still be altered in p-Pb collisions. The ratio of the spectra measured with different R provides insight to fragmentation behavior of the jet. Figure 2 shows the ratio of the $R = 0.2$ spectrum to the $R = 0.4$ spectrum for 5.02 TeV p-Pb (red circles) and for 2.76 TeV pp (black squares) collisions. The agreement between the two systems suggests that the fragmentation behavior for jets in p-Pb is very similar to that in pp collisions.

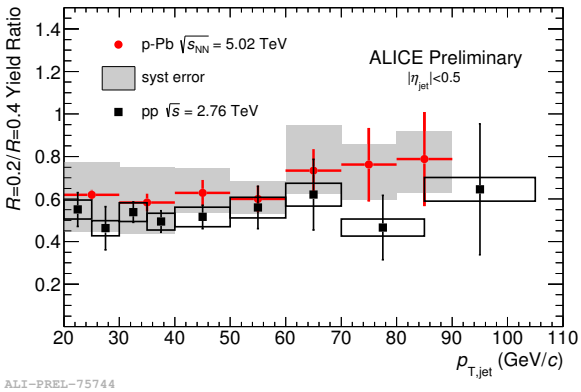

Figure 2: Cross-section ratio between $R = 0.2$ jet spectrum and $R = 0.4$ jet spectrum for fully reconstructed jets in 5.02 TeV p-Pb collisions (red circles) and 2.76 TeV pp collisions (black squares).

A more differential approach for probing the fragmentation properties of the jet is by measuring the j_T

distribution where j_T is the momentum component perpendicular to the jet axis. The measured distribution is shown in Figure 3 for two different jet momentum ranges. The distributions are compared to PYTHIA 6.4 using the CDF A tune with angular ordering on (red dashed line) and off (gray dashed line). The shape of the distribution appears to be well reproduced by the simulation. The ratio between the PYTHIA and data plotted in the lower panels of Figure 3 show better agreement when the angular ordering is turned on.

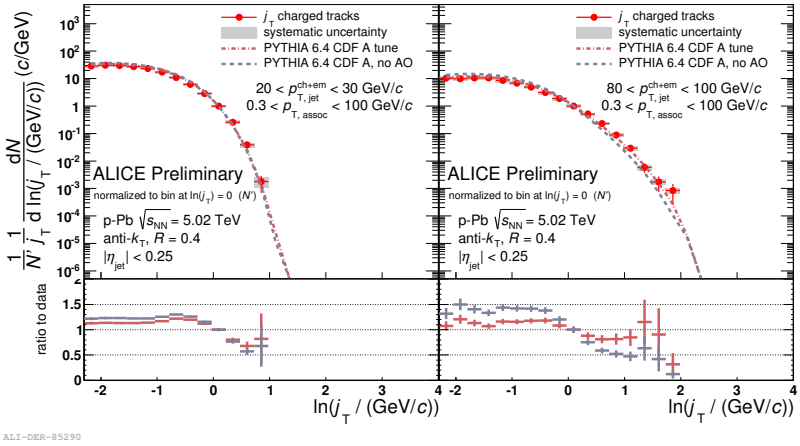

Figure 3: j_T for anti-k$_T$ $R = 0.4$ jets with $20 < p_T < 30$ GeV/c (left) and $80 < p_T < 100$ GeV/c (right) compared to PYTHIA 6.4 CDF A tune with (red) and without (gray) angular ordering (AO).

Finally, the Λ/K_s^0 ratio within a jet is measured for charged jets with $p_{T,jet}^{ch} > 10$ GeV/c and plotted in Figure 4. The plot includes jets reconstructed with the anti-k_T algorithm for different resolution parameters, R=0.2 (solid blue squares), R=0.3 (red open circles) and R=0.4 (green open squares). Little to no dependence on the resolution parameter of the jet is observed. For comparison the inclusive ratio is also plotted as solid black circles in Figure 4. The inclusive ratio is clearly larger than the ratio observed within the jet. The panels show the ratio measured in three different multiplicity classes. While the inclusive ratio appears to decrease as a function of multiplicity, the ratio measured in the jets stays constant.

In Figure 5, the data are compared to results from PYTHIA8 with Tune 4C. The inclusive Λ/K_s^0 ratio is also higher than the ratio within the jet for PYTHIA. However, the ratio within the jet agrees with the data while the data shows a clear enhancement over PYTHIA for the inclusive measurement. These results suggest that the enhancement and multiplicity dependence observed in the inclusive Λ/K_s^0 ratio does not result from a modification of the particle composition within the jets but rather is due to a change in the underlying event or soft processes.

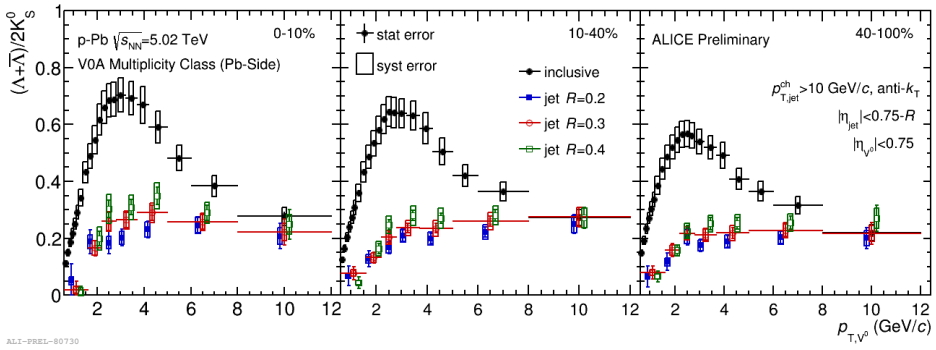

Figure 4: The Λ/K_s^0 ratio within charged jets with $p_{T,jet}^{ch} > 10$ GeV/c reconstructed for different R compared to the inclusive ratio in black for multiplicity classes 0-10% (left), 10-40% (middle) and 40-80% (right).

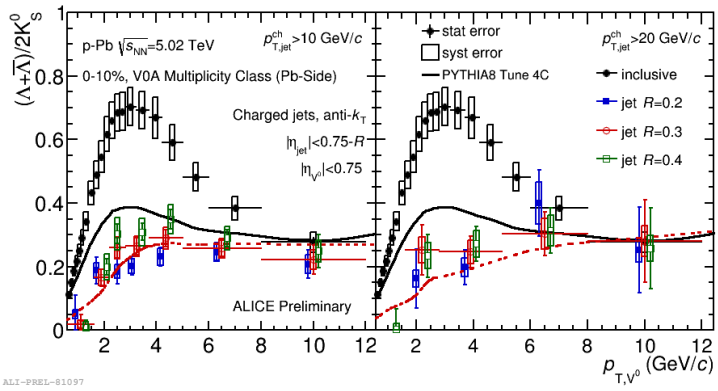

Figure 5: The inclusive Λ/K_s^0 ratio and the ratio within jets reconstructed for different R compared to PYTHIA curves for the inclusive ratio (black solid line) and ratio within R=0.3 jets (red dashed line) for charged jets with $p_{T,jet}^{ch} > 10$ GeV/c (left) and $p_{T,jet}^{ch} > 20$ GeV/c.

4 Conclusions

The fully reconstructed jet spectra for $R = 0.2$ and $R = 0.4$ have been measured by ALICE in 5.02 TeV p-Pb collisions. Comparisons to model predictions of the 5.02 TeV pp jet spectra indicate that the strong suppression observed in Pb-Pb collisions is a QGP effect and not an initial state effect. To better quantify the CNM effects, if any, on the jet spectrum, systematic uncertainties on this measurement must be reduced. In particular, the uncertainty on the reference can be reduced by measuring pp collisions at 5.02 TeV.

The ratio between spectra reconstructed with different R is consistent with the same ratio in pp collisions. This also indicates no modification to the substructure of the jets produced in p-Pb collisions. The fragmentation variable, j_T, was also measured. The agreement between the j_T distribution shape measured in p-Pb collisions and the expectations from PYTHIA also indicate no modification. The data agree best with PYTHIA when angular ordering is included.

Measurements of the Λ/K_s^0 ratio within a jet show little dependence on the resolution parameter of the jet or the multiplicity of the event and are all consistent with PYTHIA calculations. This suggests that the enhancement of the inclusive Λ/K_s^0 ratio for high multiplicity compared to low multiplicity p-Pb events is due to the underlying event or soft processes. All results presented in this talk suggest that there is no CNM effects to the production, fragmentation or particle composition of jets in p-Pb collisions.

References

[1] R. Reed (for the ALICE Collaboration), Journal of Physics: Conference Series 446 (2013) 012006 arXiv:1304.5945.

[2] ALICE Collaboration, B. Abelev, et al., Phys. Rev. Lett. 111 (2013) 222301, arXiv:1307.5530.

[3] ALICE Collaboration, B. Abelev, et al., Phys. Lett. B728 (2014) 2538. arXiv:1307.6796.

[4] ALICE Collaboration, B. Abelev, et al., Phys. Lett. B 722 (2013) 262-272, arXiv:1301.3475.

[5] M. Cacciari, G. P. Salam, G. Soyez, Eur. Phys. J. C72 (2012) 1896, arXiv:1111.6097. 012- 1896- 2.

[6] CMS Collaboration, S. Chatrchyan et al., JHEP08 (2012) 130, arXiv:hep-ex/1207.2392.

[7] X. Zhang (for the ALICE Collaboration), arXiv:1408.2672.

[8] M. Connors (for the ALICE Collaboration), arXiv:1409.3468.

[9] A. Höcker, V. Kartvelishvili, NIM A372 (1996) 469-481, arXiv:hep-ph/9509307.